Available online at www.sciencedirect.com
SCIENCE DIRECT®
PERGAMON
International Journal of Multiphase Flow 29 (2003) 621–627
International Journal of Multiphase Flow
www.elsevier.com/locate/ijmulflow

Bubble collection by a point sink in a uniform flow

J.D. Sherwood *

Schlumberger Cambridge Research, High Cross, Madingley Road, Cambridge CB3 0EL, UK

Received 11 October 2002; received in revised form 22 January 2003

Abstract

A point sink sampling device immersed in a flowing bubbly liquid collects more bubbles than would be expected on the basis of the bubble number density in the bulk fluid because the bubbles accelerate towards the sampling device faster than does the surrounding liquid. Bubble trajectories towards the sink are determined by integrating the equation of motion for the bubbles, which are assumed to be subject to pressure forces, acceleration reaction (added mass) and (possibly) drag. The number density of bubbles in the sample is predicted to be higher than that in the bulk fluid by a factor 2.37 in the absence of drag. This highlights the importance of isokinetic sampling, in which the disturbance to the streamlines is minimal. As drag increases, so bubbles tend to follow streamlines more closely and the bubble number density in the sample approaches that in the bulk fluid.

Keywords: Isokinetic sampling; Bubble trajectories

1. Introduction

If a sampling tube is inserted into a bubbly flow (Fig. 1), the velocity at which fluid is withdrawn should be as close as possible to the velocity in the bulk flow in order to minimise the disturbance to the flow. Such isokinetic sampling has been discussed by many authors, including Shires and Riley (1966), Rao and Duckler (1971), Yoshida et al. (1978), Zhang and Ishii (1995), Khor et al. (1996). Here we investigate the extent to which the number density of bubbles in the sample may differ from that in the bulk when sampling is not isokinetic and the flow is disturbed.

We consider a point sink of strength Q_0 placed at the origin in unbounded fluid which flows (in the absence of the sink) with uniform velocity $\mathbf{U}_\infty$ in the z direction. The liquid has density ρ_l and

* Tel.: +44-1223-325-363; fax: +44-1223-315-486.
E-mail address: sherwood@cambridge.oilfield.slb.com (J.D. Sherwood).

0301-9322/03/$ - see front matter
doi:10.1016/S0301-9322(03)00019-3

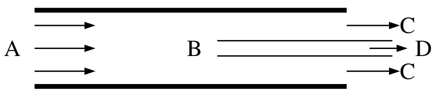

Fig. 1. For isokinetic sampling the flow rate at D is chosen to ensure minimal disturbance of the flow at B where the sample is taken.

viscosity μ. The liquid velocity $\mathbf{u}_l$ can be approximated by a linear combination of the uniform velocity and the velocity due to the sink:

$$\mathbf{u}_l = \mathbf{U}_\infty - \frac{Q_0 \mathbf{r}_s}{4\pi r_s^3} \tag{1}$$

$$= U_\infty \hat{\mathbf{z}} - \frac{Q_0(\mathbf{r} + \mathbf{z})}{4\pi (r^2 + z^2)^{3/2}} \tag{2}$$

where (r, z) are cylindrical polar coordinates with $\hat{\mathbf{z}}$ a unit vector in the z direction, and $r_s = (z^2 + r^2)^{1/2}$ is the (spherical) radial distance from the origin. Streamlines which originate at $(r, z) = (r_0, -\infty)$ will go into the sink at the origin if

$$r_0 < a = \left(\frac{Q_0}{\pi U_\infty} \right)^{1/2}. \tag{3}$$

There is a stagnation point at $(0, a/2)$, as seen in the streamlines shown in Fig. 2. This potential flow satisfies the Navier Stokes equations (Joseph and Liao, 1994), but does not, of course, satisfy the no-slip boundary condition on the walls of the sampling tube shown in Fig. 1.

We assume that the liquid contains a small volume fraction of spherical gas bubbles of radius R_0 and volume $V = \frac{4}{3}\pi R_0^3$, with negligible mass. The ambient pressure is assumed sufficiently high that any effects of gas compressibility can be neglected. Each bubble moves under the influence of pressure forces and the acceleration reaction (added mass term). We investigate the effect of drag

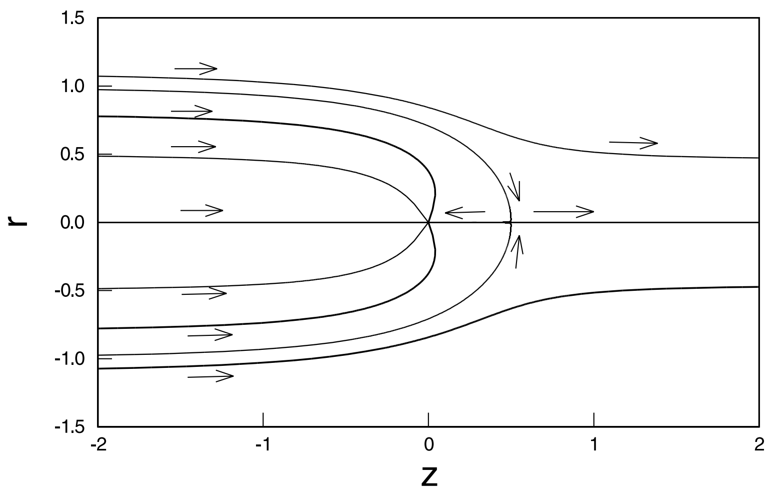

Fig. 2. Streamlines for the potential flow, with $a = 1$. The sink is at $(0, 0)$ and the stagnation point is at $(0, \frac{1}{2})$.

on the bubble by introducing a steady drag law. Thus unsteady drag forces are neglected, as are the effects of buoyancy. The forces acting on bubbles have been reviewed by Magnaudet and Eames (2000), and the analysis of the force balance presented here is similar to that of Soubiran and Sherwood (2000).

2. The equation of motion for a bubble

The bubble moves with velocity $\mathbf{v}_\mathrm{b}$. The pressure force acting on the bubble is

$$\mathbf{F}_p = V\rho_\mathrm{l}\frac{\mathrm{D}_\mathrm{l}\mathbf{u}_\mathrm{l}}{\mathrm{D}t} \tag{4}$$

where

$$\frac{\mathrm{D}_\mathrm{l}\mathbf{u}_\mathrm{l}}{\mathrm{D}t} = \frac{\partial \mathbf{u}_\mathrm{l}}{\partial t} + \mathbf{u}_\mathrm{l}\cdot\nabla\mathbf{u}_\mathrm{l} \tag{5}$$

is evaluated at the instantaneous position of the bubble. The added mass force (acceleration reaction) is

$$\mathbf{F}_\mathrm{a} = VC_m\rho_\mathrm{l}\left(\frac{\mathrm{D}_\mathrm{l}\mathbf{u}_\mathrm{l}}{\mathrm{D}t} - \frac{\mathrm{d}\mathbf{v}_\mathrm{b}}{\mathrm{d}t}\right). \tag{6}$$

We consider here that the fluid is unbounded, so that $C_m = \frac{1}{2}$. We approximate the drag force by the Levich formula for steady drag on a spherical bubble (Batchelor, 1973, p. 363)

$$\mathbf{F}_\mathrm{d} = 12\pi\mu R_0(\mathbf{u}_\mathrm{l} - \mathbf{v}_\mathrm{b}). \tag{7}$$

The equation of motion for the bubble becomes

$$\frac{\mathrm{d}\mathbf{v}_\mathrm{b}}{\mathrm{d}t} = 3\frac{\mathrm{D}_\mathrm{l}\mathbf{u}_\mathrm{l}}{\mathrm{D}t} - \frac{18\mu}{R_0^2\rho_\mathrm{l}}(\mathbf{v}_\mathrm{b} - \mathbf{u}_\mathrm{l}). \tag{8}$$

The trajectory $(r_\mathrm{b}(t), z_\mathrm{b}(t))$ of the bubble therefore satisfies

$$\frac{\mathrm{d}^2 r_\mathrm{b}}{\mathrm{d}t^2} = \left(\frac{3Q_0U_\infty}{4\pi}\right)\frac{3r_\mathrm{b}z_\mathrm{b}}{(r_\mathrm{b}^2+z_\mathrm{b}^2)^{5/2}} - \left(\frac{Q_0}{4\pi}\right)^2\frac{6r_\mathrm{b}}{(r_\mathrm{b}^2+z_\mathrm{b}^2)^3} - \frac{18\mu}{R_0^2\rho_\mathrm{l}}\left(\frac{\mathrm{d}r_\mathrm{b}}{\mathrm{d}t} + \frac{Q_0 r_\mathrm{b}}{4\pi(r_\mathrm{b}^2+z_\mathrm{b}^2)^{3/2}}\right), \tag{9a}$$

$$\begin{aligned}\frac{\mathrm{d}^2 z_\mathrm{b}}{\mathrm{d}t^2} = {} & -\left(\frac{3Q_0U_\infty}{4\pi}\right)\frac{r_\mathrm{b}^2 - 2z_\mathrm{b}^2}{(r_\mathrm{b}^2+z_\mathrm{b}^2)^{5/2}} - \left(\frac{Q_0}{4\pi}\right)^2\frac{6z_\mathrm{b}}{(r_\mathrm{b}^2+z_\mathrm{b}^2)^3} \\ & - \frac{18\mu}{R_0^2\rho_\mathrm{l}}\left(\frac{\mathrm{d}z_\mathrm{b}}{\mathrm{d}t} - U_\infty + \frac{Q_0 z_\mathrm{b}}{4\pi(r_\mathrm{b}^2+z_\mathrm{b}^2)^{3/2}}\right).\end{aligned} \tag{9b}$$

We assume that far upstream of the sampling probe the bubbles move with the velocity $\mathbf{U}_\infty$ of the liquid.

We now scale lengths by a and time by a/U_∞, and denote non-dimensional quantities by a tilde. The governing Eqs. (9) become

$$\frac{d^2\tilde{r}_b}{d\tilde{t}^2} = \frac{9\tilde{r}_b\tilde{z}_b}{4(\tilde{r}_b^2+\tilde{z}_b^2)^{5/2}} - \frac{3\tilde{r}_b}{8(\tilde{r}_b^2+\tilde{z}_b^2)^3} - M_d\left(\frac{d\tilde{r}_b}{d\tilde{t}} + \frac{\tilde{r}_b}{4(\tilde{r}_b^2+\tilde{z}_b^2)^{3/2}}\right) \tag{10a}$$

$$\frac{d^2\tilde{z}_b}{d\tilde{t}^2} = \frac{3(2\tilde{z}_b^2-\tilde{r}_b^2)}{4(\tilde{r}_b^2+\tilde{z}_b^2)^{5/2}} - \frac{3\tilde{z}_b}{8(\tilde{r}_b^2+\tilde{z}_b^2)^3} - M_d\left(\frac{d\tilde{z}_b}{d\tilde{t}} - 1 + \frac{\tilde{z}_b}{4(\tilde{r}_b^2+\tilde{z}_b^2)^{3/2}}\right) \tag{10b}$$

where

$$M_d = \frac{18\mu}{a\rho_l U_\infty}\left(\frac{a}{R_0}\right)^2. \tag{11}$$

Far upstream from the point sink, in the absence of a point sink the velocity of the bubble is

$$\left(\frac{d\tilde{r}_b}{d\tilde{t}}, \frac{d\tilde{z}_b}{d\tilde{t}}\right) = (0,1) \tag{12}$$

so that $(\tilde{r}_b, \tilde{z}_b) = (\tilde{r}_0, \tilde{t})$. When a sink is present we may evaluate the perturbation to the trajectory. Far upstream, if $M_d = 0$,

$$\tilde{r}_b = \tilde{r}_0 - \frac{3\tilde{r}_0}{8\tilde{t}^2} + O(\tilde{t}^{-3}), \quad \tilde{z}_b = \tilde{t} - \frac{3}{4\tilde{t}} + O(\tilde{t}^{-2}) \quad \tilde{t} \ll -1, \tag{13a, b}$$

with errors $O(\tilde{t}^{-5})$ in (10a) and $O(\tilde{t}^{-4})$ in (10b), leading to errors $O(\tilde{t}^{-3})$ in $\tilde{r}_b$ and $O(\tilde{t}^{-2})$ in $\tilde{z}_b$ (13a,b). However, when $M_d > 0$ the errors in expansion (13a,b) are $O(\tilde{t}^{-2})$ and $O(\tilde{t}^{-1})$ respectively. If drag is non-zero, far from the point sink the bubble tends to move with the liquid, and we instead take

$$\tilde{r}_b = \tilde{r}_0 - \frac{\tilde{r}_0}{8\tilde{t}^2} + O(M_d^{-1}t^{-3}), \quad \tilde{z}_b = \tilde{t} - \frac{1}{4t} + O(M_d^{-1}t^{-2}) \quad \tilde{t} \ll -1. \tag{14}$$

Thus (14) is an improvement upon (13a,b) unless $M_d \ll |\tilde{t}^{-1}|$. The inertia of the bubble (together with its added mass) is only one third that of the liquid it has replaced, leading to the factor 3 difference between the leading correction terms of (13a,b) and those of (14). Computations were in all cases started sufficiently far upstream for the differences between (13a,b) and (14) to be negligible.

3. Results

The governing equations (10) were integrated numerically by means of a NAG Runge–Kutta scheme. The bubble was initially far upstream, with (13a,b) as initial condition when $M_d = 0$ and (14) otherwise. It was found that $\tilde{t} = -20$ was sufficiently far upstream for results to be little affected by the precise choice of initial condition.

Fig. 3 shows trajectories when $M_d = 0$. Bubbles which start upstream at $\tilde{r}_0 \leqslant r_c = 1.538$ enter the sink. Note that there is a stagnation point, and thus a region of high pressure, at $(0, \frac{1}{2})$. Liquid slows down as it approaches the stagnation point. Bubbles are more strongly affected by the pressure gradient than is the liquid. The bubbles not only slow down, but then subsequently accelerate away from the stagnation point. In the absence of viscosity, once a bubble has started

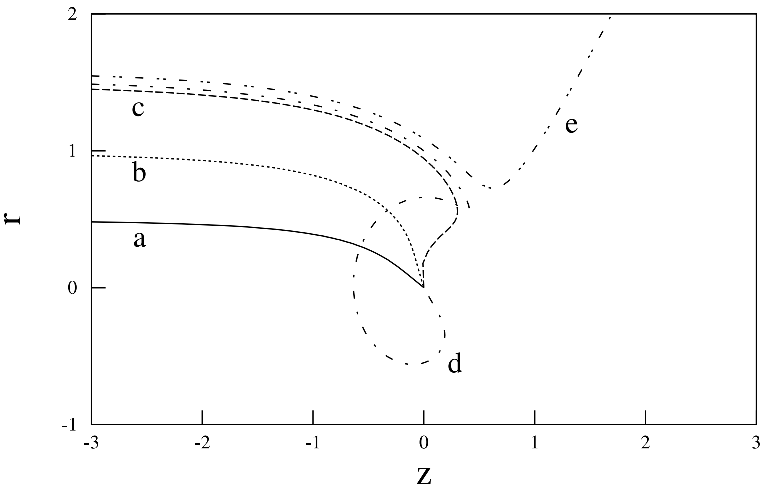

Fig. 3. Bubble trajectories, $M_d = 0$. Upstream values (a) $\tilde{r}_0 = 0.5$, (b) $\tilde{r}_0 = 1.0$, (c) $\tilde{r}_0 = 1.5$, (d) $\tilde{r}_0 = 1.538$ and (e) $\tilde{r}_0 = 1.6$.

to move away from the stagnation point along a trajectory such as (e) of Fig. 3, it continues to do so.

Fig. 4 shows bubble trajectories when $M_d = 0.2$, for the same upstream coordinates r_0 as in Fig. 3. Drag causes the bubbles to follow streamlines more closely, and only those bubbles which start upstream at $\tilde{r}_0 < r_c = 1.504$ enter the point sink. Drag ensures that any bubbles which escape the point sink eventually move with the fluid. This causes curvature of trajectories (d) and (e) towards the z direction in Fig. 4.

Fig. 5 shows how the critical upstream value r_c decreases as the drag M_d increases. We expect $r_c \to 1$ as $M_d \to \infty$. All bubbles which start upstream with $\tilde{r}_0 < r_c$ are collected, whereas only

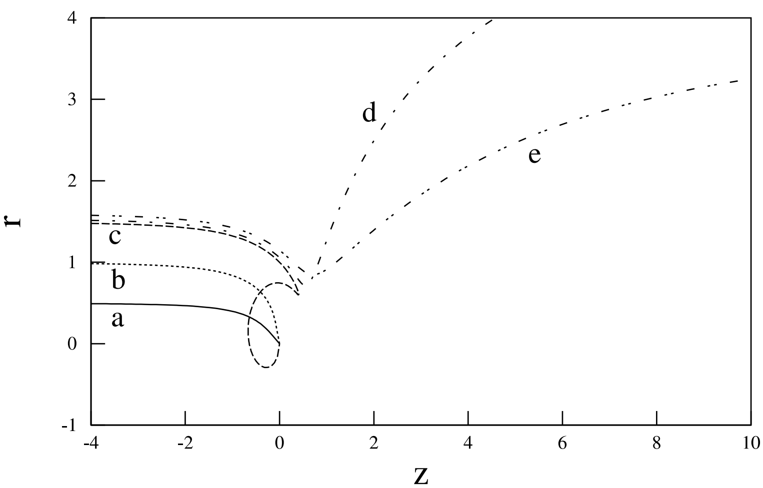

Fig. 4. Bubble trajectories, $M_d = 0.2$. Upstream values $\tilde{r}_0$ as in Fig. 3.

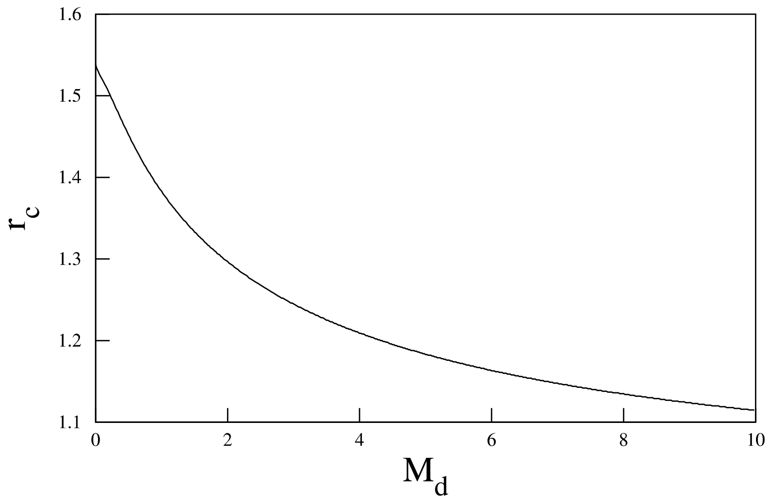

Fig. 5. The critical value r_c such that trajectories which start upstream at $\tilde{r}_0 < r_c$ enter the point sink, as a function of drag M_d.

those liquid streamlines which start upstream within $\tilde{r}_0 < 1$ enter the sampling device. If the number density of bubbles upstream is n_0, the number density of bubbles collected by the sampling device will be $n_0 r_c^2$. Thus when $M_d = 0$ the number density of bubbles in the sample will be too high by a factor $r_c^2 = 2.37$.

A real sampling device (Fig. 1) is more than just a point sink. A capillary tube (BD in Fig. 1) takes up some of the space within the pipe downstream of the sampling point. As a result, if the sampling withdrawal rate Q_0 is correctly chosen the fluid velocity in the annulus C can be unaffected by the fluid withdrawn at B (apart from effects such as viscous boundary layers on the outer walls of the sampling capillary tube). In the absence of a reduced velocity in the outer flow downstream of the sampling point, there is no adverse pressure gradient to reverse the motion of bubbles back towards the sampling point B. Moreover, upstream of the sampling point if the walls of the capillary tube are thin and the sampling velocity is correctly chosen there will be little disturbance of the fluid streamlines. If the rate at which fluid is withdrawn at B is increased, the velocity in the downstream annulus C decreases and the adverse pressure gradient will enhance the rate at which bubbles are collected. Upstream, streamlines will converge towards the orifice and bubbles trajectories will be affected even more than liquid streamlines. At a distance from the entrance large compared to the radius R_s of the sampling pipe, the flow perturbation will be close to that caused by the point-sink considered here.

The analysis has considered isolated spherical bubbles in laminar flow. Bubbles of radius R_0 must inevitable deform to enter the sampling tube of radius $R_s < R_0$, but even if the sampling tube is larger than the bubbles the strain rate $O(Q_0 R_s^{-3})$ in the neighbourhood of the entrance to the tube is likely to cause bubble deformation, since the effects of interfacial tension are typically weak. The neglect of bubble interactions requires the volume fraction of bubbles to be small not only in the bulk flow, but also in the vicinity of the probe. Close to the probe the velocity of the bubbles is higher than that of the liquid: the ratio of velocities would be $\sqrt{3}$ for radial flow towards a point sink. The increase in the bubble volume fraction close to the sampling probe is therefore less than might be expected from the enhanced rate at which bubbles are collected.

Finally, we mention solid particles of density ρ_s, which have much greater inertia than bubbles of the same size. The ratio of particle inertia to that of the surrounding fluid is characterised by the density ratio ρ_s/ρ_l. The response time for Stokes drag on the particle is $\tau_s = 2R_0^2\rho_s/9\mu$, during which time, if the typical particle velocity is U, it moves a distance of order $UR_0^2\rho_s/\mu$, which may be compared with the lengthscale a that characterises the flow field (3). Hence the ratio of the particle inertia to viscous drag forces can be expressed in terms of a modified Stokes number $S = (R_0/a)St$ where $St = UR_0\rho_s/\mu$ is the usual Stokes number (e.g. Koch and Hill, 2001). If the particles are flowing in gas of density $\rho_l \ll \rho_s$, then unless the Reynolds number for motion of the particle relative to the gas is large, the pressure force and added mass can be neglected compared to viscous drag. The gas viscosity μ is likely to be small. Unless the typical velocity U is small the Stokes number S will be large and particle inertia dominates. Only those particles which impinge upon the sampling tube will be collected. If the sampling tube is a cylinder of radius R_s, the rate of collection of solid particles will be $\pi R_s^2 U_\infty$ which is independent of the volumetric rate Q_0 at which gas is collected. Thus we require $Q_0 = \pi R_s^2 U_\infty$ if the sample is to represent the number density of particles faithfully.

If the particles are flowing in liquid, drag forces and the effect of the inertia of the continuous phase will be higher than in gas. Investigation of this case requires numerical integration of the equations for particle motion. These must now include particle inertia, which was unimportant for the bubble trajectories presented above.

References

Batchelor, G.K., 1973. An Introduction to Fluid Dynamics. Cambridge University Press, Cambridge.

Joseph, D.D., Liao, T.Y., 1994. Potential flows of viscous and viscoelastic fluids. J. Fluid Mech. 265, 1–23.

Khor, S.H., Mendes-Tatsis, M.-A., Hewitt, G.F., 1996. Application of isokinetic sampling technique in stratified multiphase flows. Proc. ASME Heat Transfer Division 3, HTD-vol. 334, pp. 101–105.

Koch, D.L., Hill, R.J., 2001. Inertial effects in suspension and porous-media flows. Annu. Rev. Fluid Mech. 33, 619–647.

Magnaudet, J., Eames, I., 2000. The motion of high-Reynolds-number bubbles in inhomogeneous flows. Annu. Rev. Fluid Mech. 32, 659–708.

Rao, C.S., Duckler, A.E., 1971. The isokinetic-momentum probe. A new technique for measurement of local voids and velocities in flow of dispersions. Ind. Eng. Chem. Fundam. 10, 520–526.

Shires, G.L., Riley, P.J., 1966. The measurement of radial voidage distribution in two-phase flow by isokinetic sampling. AEEW-M650, Winfrith.

Soubiran, J., Sherwood, J.D., 2000. Bubble motion in a potential flow within a Venturi. Int. J. Multiphase flow 26, 1771–1796.

Yoshida, H., Yamashita, K., Masuda, H., Iinoya, K., 1978. Effect of probe diameter on isokinetic sampling errors. J. Chem. Engng. Japan 11, 48–52.

Zhang, G.J., Ishii, M., 1995. Isokinetic sampling probe and image processing system for droplet measurement in two-phase flow. Int. J. Heat Mass Transfer 38, 2019–2027.